PTEP

Prog. Theor. Exp. Phys. **2018**, 063B03 (13 pages)
DOI: 10.1093/ptep/pty063

Towards entanglement of purification for conformal field theories

Hayato Hirai*, Kotaro Tamaoka*, and Tsuyoshi Yokoya*

Department of Physics, Osaka University Toyonaka, Osaka 560-0043, Japan
*E-mail: hirai@het.phys.sci.osaka-u.ac.jp, k-tamaoka@het.phys.sci.osaka-u.ac.jp, yokoya@het.phys.sci.osaka-u.ac.jp

Received April 6, 2018; Revised April 23, 2018; Accepted April 28, 2018; Published June 20, 2018

We argue that the entanglement of purification for 2D holographic conformal field theories (CFT) can be obtained from conformal blocks with internal twist operators. First, we explain our formula from the viewpoint of a tensor network model of holography. Then, we apply it to bipartite mixed states dual to a subregion of AdS_3 and the static Bañados–Teitelboim–Zanelli black hole geometries. The formula in CFT agrees with the entanglement wedge cross section in the bulk, which has been recently conjectured to be equivalent to the entanglement of purification.

Subject Index B21

1. Introduction

In the anti-de Sitter/conformal field theory (AdS/CFT) duality [1], bulk geometries have a profound connection to the quantum correlations in conformal field theories (CFT). To deepen our understanding of this interesting connection, it would be important to reveal which kind of correlation in CFT corresponds to a given geometrical object in the bulk. The best known example is the equivalence between the area of minimal surface in AdS and the entanglement entropy (EE) in CFT [2]. For mixed states, however, EE is not a very good measure for quantum entanglement because it also picks up thermal entropy. There have been several attempts to find a measure that captures just the quantum correlation for mixed states.

One such measure is the entanglement of purification (EoP) [3], which is a measure for correlation in a given bipartite mixed state. In general, we can purify a mixed state ρ_{AB} on a Hilbert space $\mathcal{H}_A \otimes \mathcal{H}_B$ to a pure state $|\psi\rangle$ on an enlarged Hilbert space $\mathcal{H}_A \otimes \mathcal{H}_B \otimes \mathcal{H}_{A'} \otimes \mathcal{H}_{B'}$. There are infinitely many methods of purification $|\psi\rangle$ such that $\rho_{AB} = \mathrm{Tr}_{A'B'} |\psi\rangle \langle\psi|$. For a given bipartite mixed state ρ_{AB}, EoP $E_\mathrm{P}(A:B)$ is defined by the minimum EE for all possible purifications:

$$E_\mathrm{P}(A:B) = \min_{\rho_{AB}=\mathrm{Tr}_{A'B'}|\psi\rangle\langle\psi|} S(\rho_{AA'}), \tag{1}$$

where $\rho_{AA'} = \mathrm{Tr}_{BB'} |\psi\rangle \langle\psi|$ and $S(\rho_{AA'})$ is EE associated with $\rho_{AA'}$. Note that for pure states EoP is equivalent to the EE since we do not need purification. It is hard to calculate EoP in practice because one needs to find an optimized solution, which minimizes the $S(\rho_{AA'})$ displayed above, from all possible purifications. In fact, there are a few examples calculating the EoP in many-body systems [4,5] and no examples directly from the definition in quantum field theory (QFT).

In this paper, we propose a formula of EoP for 2D holographic CFT [6,7] by using the replica trick [8], as well as EE. As always, we can apply this trick for EE with respect to a purified state that minimizes EE; we will call this an optimized solution $|\Psi_{\text{opt}}\rangle$:

$$E_{\text{P}}(A:B) = S(\rho_{AA'}^{(\text{opt})}) = -\text{Tr}\rho_{AA'}^{(\text{opt})} \log \rho_{AA'}^{(\text{opt})} = -\frac{\partial}{\partial n}\text{Tr}\left(\rho_{AA'}^{(\text{opt})}\right)^n\bigg|_{n\to 1}, \tag{2}$$

where $\rho_{AA'}^{(\text{opt})} = \text{Tr}_{BB'} |\Psi_{\text{opt}}\rangle \langle\Psi_{\text{opt}}|$. Once the entangling surfaces (i.e., boundary points between A' and B') are specified, one may further write this in terms of the correlation function of the (external) twist operators [9]. We argue that $\text{Tr}(\rho_{AA'}^{(\text{opt})})^n$ for holographic CFT can be well approximated as Virasoro conformal blocks, including twist operators as an intermediate state:

$$E_{\text{P}}(A:B) = -\frac{\partial}{\partial n}\mathcal{F}_{\Delta_n}\bigg|_{n\to 1}. \tag{3}$$

More information about the blocks $\mathcal{F}_{\Delta_n}$ will be explained in the following section. If one considers a mixed state, associated with the subregion of the vacuum state, the Virasoro conformal blocks further reduce to global conformal blocks. In Sect. 2, we give an interpretation of Eq. (3) from the viewpoint of a tensor network model of holography [10]. Based on the insight from this model, in Sect. 3.1, we apply our formula (3) for the aforementioned mixed state. Moreover, we also consider the EoP for the thermal state that is dual to the Bañados–Teitelboim–Zanelli (BTZ) black hole [11] in Sect. 3.2.

In particular, our computation in Sect. 3 agrees with an interesting conjecture that was recently proposed in Refs. [4,12] (see also Ref. [13]). They considered the minimal cross section of an entanglement wedge σ_{min} and defined a quantity, the "entanglement wedge cross section", by

$$E_{\text{W}} = \frac{\sigma_{\text{min}}}{4G_{\text{N}}}, \tag{4}$$

where G_{N} is Newton's constant. Their claim is that $E_{\text{P}} = E_{\text{W}}$ for CFT with the bulk dual at the leading order of large-c (large-N) expansion. Our argument in Sect. 3 gives a derivation of E_{W} within the framework of CFT. We discuss the implication of our formula and future directions in Sect. 4.

2. Some implications for EoP in AdS/CFT from the holographic code model

This section describes a heuristic justification for Eq. (3) by using the holographic code model [10]. In Sect. 2.1, we evaluate the EoP in the model and see that the $E_{\text{P}} = E_{\text{W}}$ conjecture is actually satisfied. Then in Sect. 2.1, based on the exact result of optimized purification, we argue that the EoP could be calculated in terms of the bulk two-point functions on geodesics. We will identify the two-point function with the conformal blocks in the next section.

2.1. Interpretation of the $E_{\text{P}} = E_{\text{W}}$ conjecture in the holographic code model

The holographic code model is a toy model of the AdS/CFT duality constructed by the tensor network. It captures the important relations between the bulk geometry and entanglement structures of the boundary theory; e.g., the Ryu–Takayanagi formula and he quantum error-correction feature of the boundary dual of bulk local operators in low-energy states (Hamilton–Kabat–Lifschytz–Lowe (HKLL) bulk reconstruction [14,15]). Thus, we expect that considering the interpretation of the $E_{\text{P}} = E_{\text{W}}$ conjecture in the holographic code model will help to increase our understanding of the conjecture in the AdS/CFT duality.

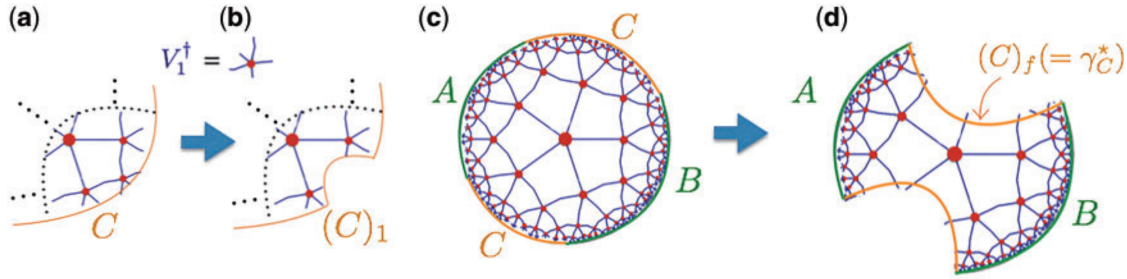

Fig. 1. (a) Part of the boundary within the tensor network (TN) of $|0\rangle$. (b) TN representation of $|\Psi\rangle_{AB(C)_1}$, which is the state cut a perfect tensor from $|0\rangle$. (c) The whole TN of $|0\rangle$. (d) The optimally purified state $|\Psi_{\text{opt}}\rangle$ constructed by iteratively cutting perfect tensors as explained in step (ii).

In the holographic code model, the duality map from bulk states to boundary states is an isometry map constructed by putting the so-called perfect tensors on the uniformly tiled 2D hyperbolic space. This isometry map is known as a "holographic code". The features of a perfect tensor ensure that this code is just a quantum error-correcting code that embeds the bulk Hilbert space into a boundary one. The non-uniqueness of the reconstruction of the bulk local operators in the boundary theory can also be understood as the well known property of the quantum error-correcting code against erasure errors. Therefore, we think of this model as a toy model of the low-energy sector of the AdS/CFT with classical geometries. Then, we assume that the bulk state is the vacuum state and the quantum bulk degrees of freedom (d.o.f.) of the tensor correspond to the d.o.f. of the quantum fields in the semiclassical theory. Although the Hamiltonian is not specified in this model, we consider the bulk vacuum state as a product state so that the Ryu–Takayanagi formula holds without quantum corrections[1].

First, we discuss the EoP in this model. Let us consider a bipartite mixed state ρ_{AB} in the boundary theory that is obtained by tracing out the d.o.f. on the boundary region $C(=\overline{AB})$ (see Fig. 1(c)). To get the EoP of ρ_{AB}, we first purify ρ_{AB}. There are many possible ways to do this, but one that minimizes the EE of $\rho_{AA'}$ must be chosen to get the EoP. It seems very difficult to choose such an optimized purification in practice, but in the holographic code model it can be done very easily. The calculation of the EoP of ρ_{AB} in this model is implemented by the following steps.

(i) Choose the original boundary pure state $|\Psi\rangle_{ABC}$, which is supposed to be the vacuum state in AdS/CFT, as the initial purification to ρ_{AB}. This state can be represented as the tensor network of Fig. 1(c). In this step, the Hilbert space associated with the d.o.f. on the boundary subregion C that is a complement to $A \cup B$ is added to the Hilbert space $\mathcal{H}_{AB}$ as a purification.

(ii) Act the Hermitian conjugate of an isometry matrix $V_1^\dagger$, which cuts the perfect tensor sitting on C:

$$V_1^\dagger|\Psi\rangle_{ABC} = |\Psi_1\rangle_{AB(C)_1}, \tag{5}$$

where $AB(C)_1$ is a new boundary obtained by removing the portion cut by the $V_1^\dagger$ from the bulk region that has ABC as its boundary (see Fig. 1(a) and (b)). Note that, in this process, $|\Psi_1\rangle_{AB(C)_1}$

[1] In the holographic code model, the HKLL-like property holds independently of the bulk state. On the other hand, if the bulk state is entangled, the Ryu–Takayanagi formula receives quantum corrections, which is the EE of the bulk state.

becomes the new purification of ρ_{AB} as follows:

$$\operatorname*{Tr}_{AB(C)_1}\Big[|\Psi_1\rangle\langle\Psi_1|\Big] = \operatorname*{Tr}_{AB(C)_1}\Big[V^\dagger V|\Psi_1\rangle\langle\Psi_1|\Big] = \operatorname*{Tr}_{ABC}\Big[|\Psi\rangle\langle\Psi|\Big] = \rho_{AB}, \tag{6}$$

where we have used $V^\dagger V = I$, which is the property of the isometry matrix, in the first equality and the cyclic property of the trace and Eq. (5) in the second equality[2]. Then, we can iterate this procedure by acting the Hermitian conjugate of the isometry matrix $V_i^\dagger$ to $|\Psi_i\rangle_{AB(C)_i}$, which maps from $\mathcal{H}_{AB(C)_i}$ to $\mathcal{H}_{AB(C)_{i+1}}$:

$$|\Psi_i\rangle_{AB(C)_i} \;\rightarrow\; |\Psi_{i+1}\rangle_{AB(C)_{i+1}} = V_i^\dagger|\Psi_i\rangle_{AB(C)_i}, \tag{7}$$

where $\mathcal{H}_{AB(C)_{i+1}}$ is defined from $\mathcal{H}_{AB(C)_i}$ in the same way as $\mathcal{H}_{AB(C)_1}$. Since the Hermitian conjugate of the isometry maps reduces the size of the Hilbert space, this procedure reduces the size of the purified Hilbert space. Thus, the entanglement of purification monotonically decreases. The boundary legs of the state $|\Psi_i\rangle$ enter deep into the bulk as the size of the purified Hilbert space reduces. This iterative procedure will terminate when the $V_f^\dagger$ acting on the $\mathcal{H}_{AB(C)_f}$ no longer exists.

(iii) After procedure (ii) ends, divide the boundary subregion $(C)_f$ into two parts, A' and B', so that A' and B' are adjacent to A and B, respectively. Then, we can obtain the density matrix $\rho_{AA'}$ by tracing out $\mathcal{H}_{BB'}$ from $|\Psi_f\rangle_{ABA'B'}$ and calculate the EE of $\rho_{AA'}$.

(iv) Iterate procedure (iii) with a different division of $(C)_f$ in order to find the optimized division, say $A'_{\min}B'_{\min}$, which minimizes the EE of $\rho_{AA'}$. Then, that minimum EE gives the EoP of ρ_{AB}.

It is very important that each step of the iterative procedure (ii) exactly corresponds to the steps of the "greedy algorithm" defined in Ref. [10], which is the algorithm to obtain the geodesics on the discretized hyperbolic space. The geodesics obtained by the algorithm are called greedy geodesics. The $A'_{\min}B'_{\min}$ end up with $\gamma_C^\star$, which is the greedy geodesic with ∂C as its boundary, namely $\partial\gamma_C^\star = \partial C$. Then, in step (iii), given the division of $(C)_f$ into A' and B', the EE of $\rho_{AA'}$ is given by the length of $\gamma_{BB'}^\star$. The optimized division is the one with the minimum length of $\gamma_{BB'}^\star$. Moreover, this optimized $\gamma_{BB'}^\star$ is exactly the entanglement wedge cross section of ρ_{AB} (Fig. 2). Eventually, the $E_{\mathrm{P}} = E_{\mathrm{W}}$ conjecture is correct in the holographic code model.

2.2. *EoP from a two-point function in the bulk*

As a result of the previous subsection, the optimally purified state $|\Psi_{\mathrm{opt}}\rangle \equiv |\Psi_f\rangle_{ABA'_{\min}B'_{\min}}$, which is the pure state in the Hilbert space associated with $ABA'_{\min}B'_{\min}$, can be written as $|\Psi_{\mathrm{opt}}\rangle = V^\dagger|0\rangle$, where $V = V_1V_2\cdots V_f$. Although this is the result in the holographic code model, let us imagine the $|\Psi_{\mathrm{opt}}\rangle$ in AdS/CFT. Namely, the bulk geometry is cut along the geodesic γ_C as in Fig. 2 and boundary

[2] To be precise, more effort is needed to justify the second equality in Eq. (6) since the sizes of the Hilbert spaces $\mathcal{H}_{ABC}$ and $\mathcal{H}_{AB(C)_1}$ are not the same. To make them the same, we add auxiliary d.o.f. $|0\rangle_{C'_1} \in \mathcal{H}_{C'_1}$ to $|\Psi_1\rangle$ such that $\mathcal{H}_{ABC} = \mathcal{H}_{AB(C)_1} \otimes \mathcal{H}_{C'_1}$. Then, both $|\Psi_1\rangle|0\rangle_{C'_1}$ and $|\Psi\rangle$ are a state in $\mathcal{H}_{ABC}$. Then, there exists the unitary operator $U : \mathcal{H}_{ABC} \rightarrow \mathcal{H}_{ABC}$ for a given V such that $V = U|0\rangle_{C'_1}$ where V is an isometry map from $\mathcal{H}_{AB(C)_1}$ to $\mathcal{H}_{ABC}$. Therefore,

$$\operatorname*{Tr}_{AB(C)_1}\Big[|\Psi_1\rangle\langle\Psi_1|\Big] = \operatorname*{Tr}_{ABC}\Big[|\Psi_1\rangle|0\rangle\langle 0|\langle\Psi_1|\Big] = \operatorname*{Tr}_{ABC}\Big[U^\dagger U|\Psi_1\rangle|0\rangle\langle 0|\langle\Psi_1|\Big] = \operatorname*{Tr}_{ABC}\Big[|\Psi\rangle\langle\Psi|\Big] = \rho_{AB}.$$

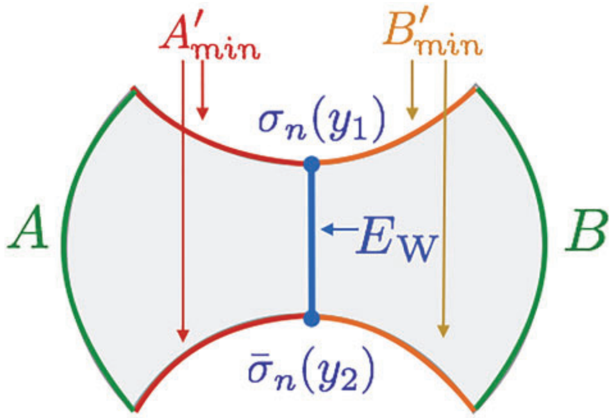

Fig. 2. The boundary space along $\gamma_C^\star$ is divided into $A'_{\rm min}$ (red line) and $B'_{\rm min}$ (orange line). y_1 and y_2 are the two boundary points between $A'_{\rm min}$ and $B'_{\rm min}$. This division is determined so that the length of the geodesic (blue line) between y_1 and y_2 becomes shortest. $E_{\rm W}$ is given by that length times $1/4G_{\rm N}$.

d.o.f. live on $ABA'_{\rm min}B'_{\rm min}$. Then $E_{\rm P}(A:B)$ would be calculated by using the replica method as

$$E_{\rm P}(A:B) = -\frac{\partial}{\partial n}\langle\Psi_{\rm opt}|\sigma_n(y_1)\bar{\sigma}_n(y_2)|\Psi_{\rm opt}\rangle\Big|_{n\to1}, \tag{8}$$

where $\sigma_n(y)$ and $\bar{\sigma}_n(y)$ are the twist operators acting on the n-sheeted boundary space along γ_C, not the original boundary on which CFT lives. y_1 and y_2 are the boundary points between $A'_{\rm min}$ and $B'_{\rm min}$ (Fig. 2). However, we cannot compute Eq. (8) directly since we do not know exactly what $|\Psi_{\rm opt}\rangle$ is in AdS/CFT. Thus, we need to put Eq. (8) into the original CFT language. This can be done by using $|\Psi_{\rm opt}\rangle = V^\dagger|0\rangle$:

$$\begin{aligned} E_{\rm P}(A:B) &= -\frac{\partial}{\partial n}\langle 0|V\sigma_n(y_1)V^\dagger V\bar{\sigma}_n(y_2)V^\dagger|0\rangle\Big|_{n\to1} \\ &= -\frac{\partial}{\partial n}\langle 0|(K\sigma_n)(y_1)(K\bar{\sigma}_n)(y_2)|0\rangle\Big|_{n\to1}, \end{aligned} \tag{9}$$

where we have defined $(K\mathcal{O})(y) \equiv V\mathcal{O}(y)V^\dagger$. Although we do not know the concrete expression of V in AdS/CFT, $(K\mathcal{O})(y)$ is the boundary operator that is dual to the bulk local operator $\mathcal{O}(y)$ in the holographic code model[3]. Therefore, it would be natural to think of the $(K\mathcal{O})(y)$ in AdS/CFT as a non-local operator on the boundary along C that is constructed by the HKLL bulk reconstruction of the bulk local operator $\mathcal{O}^{\rm (bulk)}(y)$. Thus, in the bulk language, Eq. (9) can be written as

$$E_{\rm P}(A:B) = -\frac{\partial}{\partial n}\langle 0_{\rm AdS}|\sigma_n^{\rm (bulk)}(y_1)\bar{\sigma}_n^{\rm (bulk)}(y_2)|0_{\rm AdS}\rangle\Big|_{n\to1}, \tag{10}$$

where $\sigma_n^{\rm (bulk)}$ and $\bar{\sigma}_n^{\rm (bulk)}$ are the bulk dual of the twist operators σ_n and $\bar{\sigma}_n$, respectively, with their mass $m^2 = \Delta_n(\Delta_n - 2)$. Here, Δ_n ($\bar{\Delta}_n$) is the scaling dimension of σ_n ($\bar{\sigma}_n$). In the next section, we

[3] Strictly speaking, in the holographic code model, $(K\mathcal{O})(y)$ is not the boundary operator dual to the bulk operator $\sigma_n^{\rm (bulk)}(y)$ but the boundary operator dual to $\sigma_n(y)$, acting on the boundary cut along $\gamma_C^\star$. $\sigma_n(y)$ and $\sigma_n^{\rm (bulk)}(y)$ act on a bulk leg and a boundary leg of the same perfect tensor on $\gamma_C^\star$, respectively. We need $\sigma_n(y)$ acting on at least three legs of the perfect tensor to reconstruct the bulk local (one-body) operator $\sigma_n^{\rm (bulk)}(y)$, which should be understood as a discretized version of the bulk reconstruction. However, we do not distinguish between them since these operators are identified up to the scaling factor in AdS/CFT.

will see that Eq. (10) agrees with the E_W of AB in the large-c limit and this can be expressed in terms of the global conformal block in CFT.

3. Entanglement wedge cross section from holographic CFT

In this section, we argue that the right-hand side of Eq. (10) can be obtained from conformal blocks (CBs) including twist operators as intermediate states. With the previous argument in Sect. 2, we can regard it as EoP for holographic CFT. CBs are the basis of correlation functions in CFT. These are determined purely from the conformal symmetry and irreducible representations thereof. We have an interesting integral representation of the CB, dubbed the geodesic Witten diagram (GWD) [16,17]. Remarkably, one can apply this representation for arbitrary CFT even with no bulk dual. Taking the large-c limit, we can read off the entanglement wedge cross section from GWD, as discussed below.

3.1. *Cross section of AdS_3 from the global conformal block*

Firstly, we extract the right-hand side of Eq. (10) in AdS_3 from CB with internal twist operators. Let us consider CB associated with the following four-point function:

$$\langle 0|\mathcal{O}_{1\mathrm{L}}(\phi_1)\mathcal{O}_{2\mathrm{L}}(\phi_2)\mathcal{O}_{3\mathrm{L}}(\phi_3)\mathcal{O}_{4\mathrm{L}}(\phi_4)|0\rangle\,. \tag{11}$$

Hereafter we will assume that the scaling dimensions of the $\mathcal{O}_{i\mathrm{L}}$ ($i = 1, 2, 3, 4$) are the same. We will consider the specific channel in which $\mathcal{O}_{1\mathrm{L}}\mathcal{O}_{4\mathrm{L}}$ fuses into σ_n and $\mathcal{O}_{2\mathrm{L}}\mathcal{O}_{3\mathrm{L}}$ into $\bar{\sigma}_n$. Since we apply the replica trick, we are not considering the original CFT $\mathcal{C}$ but its cyclic orbifold $\mathcal{C}^n/\mathbb{Z}_n$. In the large-$c$ holographic CFT, the contribution of the channel mentioned above will be dominant for the original four-point function (11) since the conformal dimension of twist operators is the lowest one in the sector with twist number ± 1 and its spectrum is sparse[4]. More detailed properties of $O_{i\mathrm{L}}$ will be discussed in Sect. 4. We will briefly discuss the global CB G_{Δ_n} associated with the twist operators, but it turns out to be the same as Virasoro CB $\mathcal{F}_{\Delta_n}$ at the semiclassical limit below. We shall consider CFT_2 on the cylinder for simplicity. Then, in the bulk side, it is dual to global AdS_3:

$$ds^2 = \frac{1}{\cos^2\rho}\left(d\rho^2 - dt^2 + \sin^2\rho\, d\phi^2\right). \tag{12}$$

We have a boundary cylinder at $\rho = \frac{\pi}{2}$ on which CFT_2 lives. On the fixed time slice $t = 0$, GWD is given by[5]

$$G_{\Delta_n}(u,v) = \int_{\gamma_{14}} d\lambda \int_{\gamma_{23}} d\lambda' G^{\Delta_n}_{bb}(y(\lambda), y'(\lambda')), \tag{13}$$

where $G^{\Delta_n}_{bb}(y, y')$ is the scalar bulk–bulk propagator in AdS_3 with mass $m^2 = \Delta_n(\Delta_n - 2)$. The explicit form of the propagator is given in Appendix A. In general, GWD includes a bulk–boundary propagator. However, under our assumption about the scaling dimension of the external operators, it reduces to Eq. (13). This is because CB depends only on the difference of external scaling dimensions

[4] In unitary CFT, the twist operators have the lowest scaling dimension in the sectors with twist number ± 1; hence, these are the "vacuum" states on the sectors via the operator/state map. Moreover, the other primary states in these sectors are systematically built from the primary operators in the original CFT $\mathcal{C}$ acting on these "vacua" [18].

[5] Note that we are not discussing conformal partial waves but rather conformal blocks.

for each OPE. Each end point y, y' in Eq. (13) is sitting on each geodesic γ_{14} and γ_{23}. Here we denote γ_{ij} as the geodesic anchored on the boundary points ϕ_i and ϕ_j.

Let us take the semiclassical limit, i.e., the large-c limit, leaving Δ_n/c fixed. We will apply the following argument to the twist operators $\sigma_n, \bar{\sigma}_n$ with scaling dimension $\Delta_n = \frac{c}{12}(n - \frac{1}{n})$. In this limit, we can use the saddle-point approximation for the integrand. At the leading order of the approximation, Eq. (13) reduces to

$$G_{\Delta_n}(u, v) = e^{-\Delta_n \sigma_{\min}(u,v)}, \tag{14}$$

where $\sigma_{\min}$ is the minimum length between two geodesics. For the explicit form of $\sigma_{\min}$, see Appendix A. $\sigma_{\min}$ is determined purely from the cross ratios, as CB is; hence, it is conformally invariant. Notice that the dominant contribution in the approximation (14) obviously comes from the bulk–bulk propagator stretched over two geodesics such that it minimizes the distance between two end points. Moreover, under the limit $n \to 1$, we can regard $\sigma_n, \bar{\sigma}_n$ as light operators. Then, the difference between the global CB G_{Δ_n} and the Virasoro one $\mathcal{F}_{\Delta_n}$ becomes negligible [19]. Therefore, we can identify the Virasoro CB $\mathcal{F}_{\Delta_n}$ with the two-point function in Eq. (10):

$$\mathcal{F}_{\Delta_n} = \langle 0_{\mathrm{AdS}} |\, \sigma_n^{(\mathrm{bulk})}(y_1) \bar{\sigma}_n^{(\mathrm{bulk})}(y_2)\, | 0_{\mathrm{AdS}} \rangle. \tag{15}$$

Eventually, we obtain

$$-\frac{\partial}{\partial n} \mathcal{F}_{\Delta_n}(u, v) \bigg|_{n \to 1} = \frac{c}{6} \sigma_{\min} = E_{\mathrm{W}}. \tag{16}$$

It is worth stressing that we have extracted the entanglement wedge cross section within the CFT framework.

3.2. *Cross section of BTZ black hole from conformal blocks*

Next, we derive the entanglement wedge cross section of a BTZ black hole [11] from the semiclassical Virasoro CBs. For simplicity, we will only consider the static case. The metric of a static BTZ black hole with mass M is given by

$$ds^2 = \frac{\alpha^2}{\cos^2 \rho} \left(\frac{d\rho^2}{\alpha^2} - dt^2 + \sin^2 \rho d\phi^2 \right), \tag{17}$$

where α^2 is defined as

$$\alpha^2 \equiv -8 G_{\mathrm{N}} M < 0. \tag{18}$$

It is well known that the above metric can be obtained from the global AdS_3 one (12) with a coordinate transformation $(t, \phi) \mapsto (\alpha t, \alpha \phi)$.

3.2.1. *Similar phase to global AdS_3*

Let us first consider the case when the entanglement wedge does not cover the black hole (see the left-hand side of Fig. 3). In this case, we can follow the previous argument for global AdS_3 and conclude that EoP can be obtained from the bulk–bulk propagator on the geodesics of a BTZ black hole. Hence, one can simply obtain EoP in this case from the coordinate transformation of Eq. (16). Moreover, this argument can be translated into the transformation of CB. Namely, we can use the

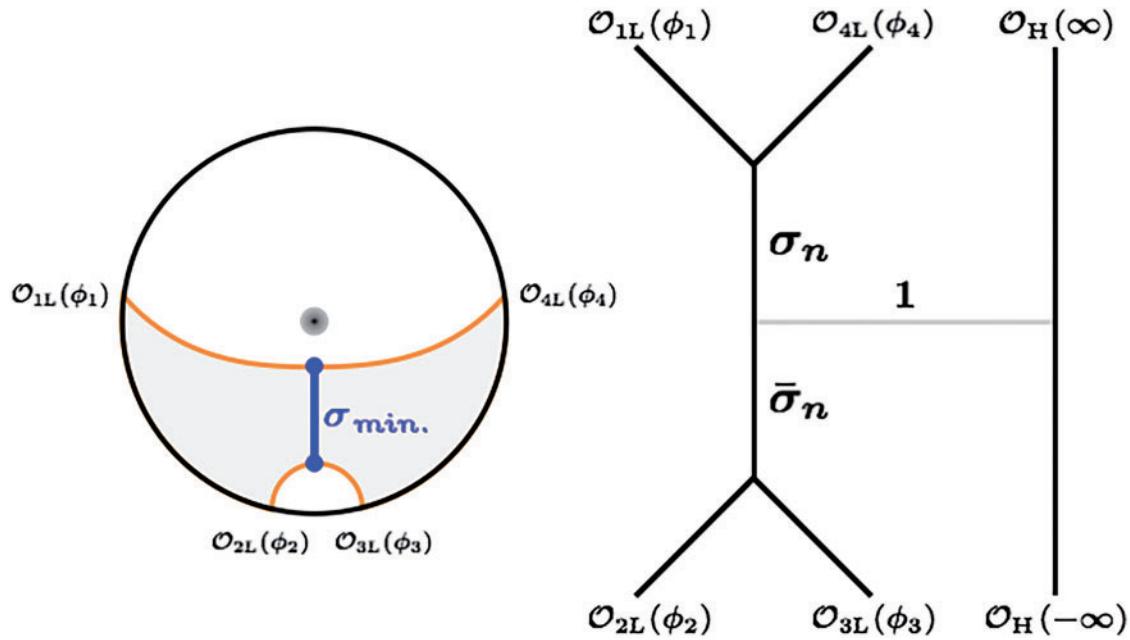

Fig. 3. Left: an entanglement wedge (shaded region) for a BTZ black hole. In this situation, the wedge does not cover the black hole horizon (black point in the center). Here we consider a time slice $t = 0$. The blue solid line represents the minimal cross section. Right: related OPE channel for the left diagram. Since we take the semiclassical heavy–light limit, the identity exchange becomes factorized. Hence, it reduces to the four-point global CB with a coordinate transformation $\phi' = \alpha\phi$.

fact that the heavy–light Virasoro CB can be obtained from the global CB in the previous subsection with a coordinate transformation $(\phi', \tau') = (\alpha\phi, \alpha\tau)$ for the external light operators [20].

In what follows, we will be more precise about our setup. We are now considering the semiclassical heavy–light Virasoro CBs (heavy–light CBs, for brevity) associated with the following six-point correlator:

$$\langle 0|\mathcal{O}_{\rm H}(\infty)\mathcal{O}_{\rm H}(-\infty)\mathcal{O}_{1\rm L}(\phi_1)\mathcal{O}_{2\rm L}(\phi_2)\mathcal{O}_{3\rm L}(\phi_3)\mathcal{O}_{4\rm L}(\phi_4)|0\rangle. \tag{19}$$

Since we are considering the time slice of the boundary of Eq. (17), we write each point of the cylinder as ϕ_i. Here heavy operators $\mathcal{O}_{\rm H}$ have a scaling dimension $\Delta_{\rm H} \sim c$ that can be identified with a pure state behaving like a BTZ black hole[6]. One could regard the state $|\mathcal{O}_{\rm H}\rangle$ as a purification of the original thermal state. On the other hand, the scaling dimension of the light operator $\mathcal{O}_{i\rm L}$ denoted by $\Delta_{i\rm L}$ is small enough under the large-c limit (again, we assume that the $\Delta_{i\rm L}$ are the same). More precisely, we will assume $\Delta_{i\rm L}/c \ll 1$ so that the $\mathcal{O}_{i\rm L}$ can probe the BTZ geometry without any back reaction [22]. Again, this condition will be satisfied since the Δ_n becomes small under the limit $n \to 1$. After the transformation and the semiclassical limit, all contributions of CB other than the global sectors become negligible at the leading order of the large-c limit.

This is a generic argument for heavy–light CBs, but let us focus on the OPE channel in which the $\mathcal{O}_{\rm H}$ fuse into the identity operator (and its Virasoro descendants). Then, our heavy–light CB, say $\mathcal{F}^{(6)}_{\Delta_n}$, reduces to a four-point global CB with a coordinate transformation (times $\langle\mathcal{O}_{\rm H}(\infty)\mathcal{O}_{\rm H}(-\infty)\rangle$,

[6] We can relate $\Delta_{\rm H}$ to α such that $\alpha^2 = 1 - \frac{12\Delta_{\rm H}}{c}$. Here c is the central charge identified with $c \equiv \frac{3}{2G_{\rm N}}$ on the gravity side [21].

which is normalized). We are interested in the case in which the remaining two pairs of $\mathcal{O}_{i\mathrm{L}}$ fuse into the twist operators; see the right-hand panel of Fig. 3. After all, $\mathcal{F}^{(6)}_{\Delta_n}$ reduces to a four-point global CB on the new coordinates $\phi' = \alpha\phi$. Evaluating Eq. (13) in the new coordinates with the saddle-point approximation for Δ_n, we have obtained

$$\mathcal{F}^{(6)}_{\Delta_n}(u, v) \sim e^{-\Delta_n \sigma_{\min}(u,v)}, \tag{20}$$

where $\sigma_{\min}(u, v)$ matches the entanglement wedge cross section of BTZ geometry (blue solid line in the left-hand panel of Fig. 3; see also Appendix A).

3.2.2. A new phase: sections touching the horizon

There is another phase of the entanglement wedge that covers the horizon. In this case, a rigorous GWD expression of the six-point CB has not yet been produced. On the other hand, it is known that the heavy–light CBs can be obtained from a different method, called the world-line approach [23] (see also Refs. [24–26]). In particular, the six-point heavy–light CB in Fig. 4 becomes a product of the four-point ones [26]:

$$\mathcal{F}^{(6)}(\Delta_n, \Delta_{\mathrm{H}}, c, \phi_i) = \mathcal{F}^{(4)}_{\Delta_n}(\Delta_{\mathrm{H}}, c, \phi_{14})\mathcal{F}^{(4)}_{\Delta_n}(\Delta_{\mathrm{H}}, c, \phi_{23}). \tag{21}$$

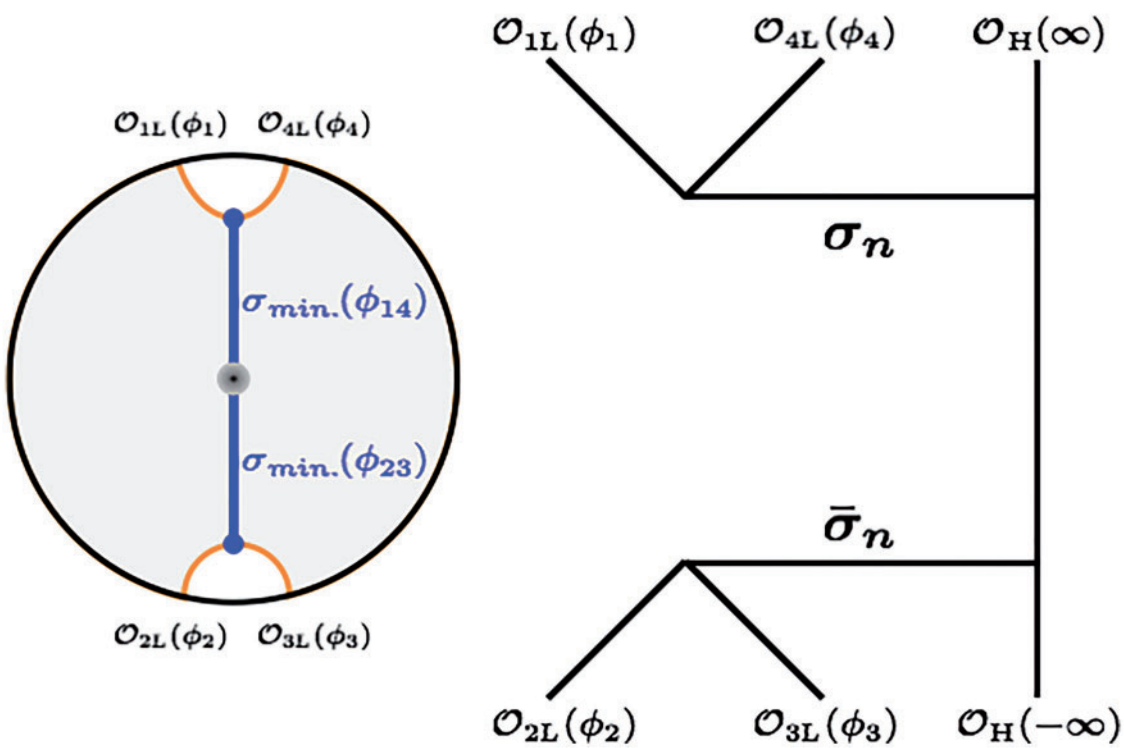

Fig. 4. For sufficiently large subsystems, an entanglement wedge covers the black hole horizon. In this case, the entanglement wedge cross section becomes the blue solid lines $\sigma_{\min}(\phi_{14}) + \sigma_{\min}(\phi_{23})$ in the left-hand figure. Right: the related OPE channel. Under the appropriate limit, the corresponding six-point heavy–light CB becomes equivalent to the product of two four-point heavy–light CBs. Each of the CBs produces one of two cross sections, $\sigma_{\min}(\phi_{14})$ or $\sigma_{\min}(\phi_{23})$.

Here the $\mathcal{F}^{(4)}_{\Delta_n}$ are four-point heavy–light CBs[7]. The above equality (21) is verified only when the saddle-point approximation can be applied:

$$\mathcal{F}^{(4)}_{\Delta_n}(\Delta_{\mathrm{L}}, \Delta_{\mathrm{H}}, \alpha, \phi_{ij}) \sim e^{-\Delta_n \sigma_{\min}(\phi_{ij})}. \tag{22}$$

This situation is just what we want to consider. In the end, we get

$$-\frac{\partial}{\partial n}\left(\mathcal{F}^{(6)}(\Delta_n, \Delta_{\mathrm{L}}, \Delta'_{\mathrm{L}}, \Delta_{\mathrm{H}}, c, \phi_i)\right)\Big|_{n\to 1} = \frac{c}{6}\left(\sigma_{\min}(\phi_{14}) + \sigma_{\min}(\phi_{23})\right), \tag{23}$$

where

$$\sigma_{\min}(\phi_{ij}) = \log\left|\frac{\cos\frac{\alpha\phi_{ij}}{4}}{\sin\frac{\alpha\phi_{ij}}{4}}\right|. \tag{24}$$

The right-hand side of Eq. (23) is nothing but the entanglement wedge cross section in the left panel of Fig. 4.

Before closing this section, we briefly mention the case of the two-sided eternal black hole [27]. The bulk computation has been discussed in Ref. [4]. If the two boundary regions, A and B, are on different sides, then the entanglement wedge cross section is inhaled by the horizon and does not cover the entire black hole. It would be interesting to search for its counterpart in the boundary, but we leave this for future work.

4. Summary and discussion

In this paper, we have proposed a formula (3) for EoP in 2D holographic CFT. We explained the validity of Eq. (3) with the aid of the holographic code model in Sect. 2. Moreover, our formula reproduces the entanglement wedge cross section in a time slice of the AdS_3 and one of the static BTZ black holes. We observed this agreement in Sect. 3.

From the argument in Sect. 2.2, we could not specify the external operators $\mathcal{O}_{i\mathrm{L}}$ $(i = 1, 2, 3, 4)$ in Sect. 3, but at least the twist number must be conserved modulo n in each OPE. Since the twist operator $\sigma_n(\bar{\sigma}_n)$ belongs to the twisted sector with twist number ± 1, one possibility might be that the $O_{i\mathrm{L}}$ belongs to the sector with twist number $\pm\frac{n+1}{2}$, where n is supposed to be an odd integer before the analytic continuation of n. If so, a correlation function like Eq. (11) could explain why the $\mathcal{O}(c)$ contribution of EoP vanishes under the transition from the entanglement wedge to the causal one. Namely, if we take another OPE channel with fixed external operators, the above internal twist operators cannot be produced due to the twist number conservation. The relation between the causal/entanglement wedge and OPE channels is reminiscent of the one for holographic mutual information. Identifying external operators in holographic CFT may provide a clue for EoP in more generic QFT.

We have focused on 2D CFT and its bulk dual. One may be curious about its extension to higher dimensions. Since the twist operators in higher dimensions become non-local, generalization of our argument is not so straightforward. At least the $E_{\mathrm{P}} = E_{\mathrm{W}}$ conjecture can still work even in higher dimensions, so it will be fruitful to study the higher-dimensional counterpart of our $\sigma_n^{(\mathrm{bulk})}$ in Sect. 2.

[7] Our convention of the Virasoro conformal blocks is different from Ref. [26] and so forth. We are just using the terminology "conformal blocks" so that it depends only on the cross ratio.

Since our insight and optimization were based on the holographic code model, we are still assuming some holography. In particular, we do not say that our argument proves $E_{\rm P} = E_{\rm W}$ even for holographic CFT. For further verification of Eq. (3), we need to consider optimization within the framework of field theories. To this end, it would be very useful to utilize cMERA [28] or a path-integral approach like Ref. [29]. However, at the very least, the right-hand side of Eq. (3) defines a quantity of correlation measure in CFT that indeed agrees with the entanglement wedge cross section at the large-c limit. Therefore, it would be very interesting to study Eq. (3) further with the $1/c$ corrections and its time dependence.

It is also promising to see the connection of EoP to the kinematic space [30] since conformal blocks can be regarded as a two-point function of the OPE blocks [31,32]. We leave these questions for future work.

Acknowledgements

We are grateful to Tokiro Numasawa, Tadashi Takayanagi, and Satoshi Yamaguchi for valuable comments and discussions. K.T. would like to thank the organizers of the workshop "Holography, Quantum Entanglement and Higher Spin Gravity II", where part of this work was presented.

Funding

Open Access funding: SCOAP[3].

Appendix A. Explicit form of the propagator and minimal geodesic length

In this appendix, we note some explicit forms of the quantities displayed in Sect. 3. The bulk–bulk propagator $G^{\Delta_p}_{bb}(y, y')$ (in AdS_3) is

$$G^{\Delta_p}_{bb}(y, y') = \frac{e^{-\Delta_p \sigma(y,y')}}{1 - e^{-2\sigma(y,y')}}. \tag{A.1}$$

Here $\sigma(y, y')$ is the geodesic distance between y and y',

$$\sigma(y, y') = \log\left(\frac{1 + \sqrt{1 - \xi^2}}{\xi}\right), \quad \xi = \frac{\cos\rho\cos\rho'}{\cos(t - t') - \sin\rho\sin\rho'\cos(\phi - \phi')}, \tag{A.2}$$

where we take the global coordinates (12). The geodesics γ_{ij} anchored on the boundary points $(\phi_i, t_i = 0)$ and $(\phi_j, t_j = 0)$ are given by

$$\cos\rho(\lambda) = \frac{\left|\sin\frac{\phi_{ij}}{2}\right|}{\cosh\lambda}, \tag{A.3a}$$

$$e^{2i\phi(\lambda)} = \frac{\cosh\left(\lambda - \frac{i\phi_{ij}}{2}\right)}{\cosh\left(\lambda + \frac{i\phi_{ij}}{2}\right)} e^{i(\phi_i + \phi_j)}, \tag{A.3b}$$

where λ is a proper distance for the geodesic and $\phi_{ij} = \phi_i - \phi_j$.

The minimum length between two geodesics $\sigma_{\min}$ in Eq. (14) is given by the cross ratio u, v,

$$\sigma_{\min}(u, v) = \log\left(\frac{1 + \sqrt{u} + \sqrt{(1 + \sqrt{u})^2 - v}}{\sqrt{v}}\right), \tag{A.4}$$

where

$$u = \frac{P_{12}P_{34}}{P_{13}P_{24}}, \quad v = \frac{P_{23}P_{14}}{P_{13}P_{24}}. \tag{A.5}$$

Here P_{ij} (on a time slice $t = 0$) is

$$P_{ij} = 4\sin^2\left(\frac{\phi_{ij}}{2}\right), \tag{A.6}$$

for global AdS_3. One can also obtain σ_{min} for static BTZ black holes in Sect. 3.2.1 by replacing P_{ij} with $P_{ij}^{(\alpha)}$,

$$P_{ij}^{(\alpha)} = 4\sin^2\left(\frac{\alpha}{2}\phi_{ij}\right), \tag{A.7}$$

where α is a pure imaginary number defined in Eq. (18).

References

[1] J. Maldacena, Int. J. Theor. Phys. **38**, 1113 (1999) [Adv. Theor. Math. Phys. **2**, 231 (1998)] [arXiv:hep-th/9711200] [Search INSPIRE].
[2] S. Ryu and T. Takayanagi, Phys. Rev. Lett. **96**, 181602 (2006) [arXiv:hep-th/0603001] [Search INSPIRE].
[3] B. M. Terhal, M. Horodecki, D. W. Leung, and D. P. DiVincenzo, J. Math. Phys. **43**, 4286 (2002) [arXiv:quant-ph/0202044].
[4] P. Nguyen, T. Devakul, M. G. Halbasch, M. P. Zaletel, and B. Swingle, J. High Energy Phys. **1801**, 098 (2018) [arXiv:1709.07424 [hep-th]] [Search INSPIRE].
[5] A. Bhattacharyya, T. Takayanagi, and K. Umemoto, J. High Energy Phys. **1804**, 132 (2018) [arXiv:1802.09545 [hep-th]] [Search INSPIRE].
[6] I. Heemskerk, J. Penedones, J. Polchinski, and J. Sully, J. High Energy Phys. **0910**, 079 (2009) [arXiv:0907.0151 [hep-th]] [Search INSPIRE].
[7] S. El-Showk and K. Papadodimas, J. High Energy Phys. **1210**, 106 (2012) [arXiv:1101.4163 [hep-th]] [Search INSPIRE].
[8] C. Callan and F. Wilczek, Phys. Lett. B **333**, 55 (1994) [arXiv:hep-th/9401072] [Search INSPIRE].
[9] P. Calabrese and J. Cardy, J. Stat. Mech. **0406**, P06002 (2004) [arXiv:hep-th/0405152] [Search INSPIRE].
[10] F. Pastawski, B. Yoshida, D. Harlow, and J. Preskill, J. High Energy Phys. **1506**, 149 (2015) [arXiv:1503.06237 [hep-th]] [Search INSPIRE].
[11] M. Bañados, C. Teitelboim, and J. Zanelli, Phys. Rev. Lett. **69**, 1849 (1992) [arXiv:hep-th/9204099] [Search INSPIRE].
[12] T. Takayanagi and K. Umemoto, arXiv:1708.09393 [hep-th] [Search INSPIRE].
[13] N. Bao and I. F. Halpern, J. High Energy Phys. **1803**, 006 (2018) [arXiv:1710.07643 [hep-th]] [Search INSPIRE].
[14] A. Hamilton, D. Kabat, G. Lifschytz, and D. A. Lowe, Phys. Rev. D **74**, 066009 (2006) [arXiv:hep-th/0606141] [Search INSPIRE].
[15] A. Almheiri, X. Dong, and D. Harlow, J. High Energy Phys. **1504**, 163 (2015) [arXiv:1411.7041 [hep-th]] [Search INSPIRE].
[16] E. Hijano, P. Kraus, E. Perlmutter, and R. Snively, J. High Energy Phys. **1601**, 146 (2016) [arXiv:1508.00501 [hep-th]] [Search INSPIRE].
[17] E. Hijano, P. Kraus, E. Perlmutter, and R. Snively, J. High Energy Phys. **1512**, 077 (2015) [arXiv:1508.04987 [hep-th]] [Search INSPIRE].
[18] L. Borisov, M. B. Halpern, and C. Schweigert, Int. J. Mod. Phys. A **13**, 125 (1998) [arXiv:hep-th/9701061] [Search INSPIRE].
[19] A. L. Fitzpatrick, J. Kaplan, and M. T. Walters, J. High Energy Phys. **1408**, 145 (2014) [arXiv:1403.6829 [hep-th]] [Search INSPIRE].
[20] A. L. Fitzpatrick, J. Kaplan, and M. T. Walters, J. High Energy Phys. **1511**, 200 (2015) [arXiv:1501.05315 [hep-th]] [Search INSPIRE].
[21] J. D. Brown and M. Henneaux, Commun. Math. Phys. **104**, 207 (1986).

[22] C. T. Asplund, A. Bernamonti, F. Galli, and T. Hartman, J. High Energy Phys. **1502**, 171 (2015) [arXiv:1410.1392 [hep-th]] [Search INSPIRE].
[23] E. Hijano, P. Kraus, and R. Snively, J. High Energy Phys. **1507**, 131 (2015) [arXiv:1501.02260 [hep-th]] [Search INSPIRE].
[24] K. Alkalaev and V. Belavin, J. High Energy Phys. **1508**, 049 (2015) [arXiv:1504.05943 [hep-th]] [Search INSPIRE].
[25] K. Alkalaev and V. Belavin, Nucl. Phys. B **904**, 367 (2016) [arXiv:1510.06685 [hep-th]] [Search INSPIRE].
[26] P. Banerjee, S. Datta, and R. Sinha, J. High Energy Phys. **1605**, 127 (2016) [arXiv:1601.06794 [hep-th]] [Search INSPIRE].
[27] J. Maldacena, J. High Energy Phys. **0304**, 021 (2003) [arXiv:hep-th/0106112] [Search INSPIRE].
[28] J. Haegeman, T. J. Osborne, H. Verschelde, and F. Verstraete, Phys. Rev. Lett. **110**, 100402 (2013) [arXiv:1102.5524 [hep-th]] [Search INSPIRE].
[29] P. Caputa, N. Kundu, M. Miyaji, T. Takayanagi, and K. Watanabe, Phys. Rev. Lett. **119**, 071602 (2017) [arXiv:1703.00456 [hep-th]] [Search INSPIRE].
[30] B. Czech, L. Lamprou, S. McCandlish, and J. Sully, J. High Energy Phys. **1510**, 175 (2015) [arXiv:1505.05515 [hep-th]] [Search INSPIRE].
[31] B. Czech, L. Lamprou, S. McCandlish, B. Mosk, and J. Sully, J. High Energy Phys. **1607**, 129 (2016) [arXiv:1604.03110 [hep-th]] [Search INSPIRE].
[32] J. de Boer, F. M. Haehl, M. P. Heller, and R. C. Myers, J. High Energy Phys. **1608**, 162 (2016) [arXiv:1606.03307 [hep-th]] [Search INSPIRE].